Multimodal Action of Single Na^+ Channels in Myocardial Mouse Cells

Thomas Böhle and Klaus Benndorf
Department of Physiology, University of Cologne, D-50931 Cologne, Germany

ABSTRACT Unitary Na^+ currents of myocardial mouse cells were studied at room temperature in 10 cell-attached patches, each containing one and only one channel. Small-pore patch pipettes (resistance 10–97 MΩ when filled with 200% Tyrode's solution) with exceptionally thick walls were used. Observed were both rapidly inactivating (6 patches) and slowly inactivating (3 patches) Na^+ currents. In one patch, a slow transition from rather fast to slow inactivation was detected over a time of 0.5 h. A short and a long component of the open-channel life time were recorded at the beginning, but only a short one at the end of the experiment. Concomitantly, the first latency was slowed. Amplitude histograms showed that the electrochemical driving force across the pore of the channel did not change during this time. In three patches, a fast and repetitive switching between different modes of Na^+ channel action could be clearly identified by plotting the long-time course of the averaged current per trace. The ensemble-averaged current formed in each mode was different in kinetics and amplitude. Each mode had a characteristic mean open-channel life time and distribution of first latency, but the predominant single-channel current amplitude was unaffected by mode switches. It is concluded that two types of changes in kinetics may happen in a single Na^+ channel: fast and reversible switches between different modes, and a slow loss of inactivation.

INTRODUCTION

Besides typically fast-inactivating Na^+ currents (Hodgkin and Huxley, 1952), which are found in nearly all excitable tissues, also persistent Na^+ currents have been detected in skeletal muscle (Patlak and Ortiz, 1986, 1989; Gage et al., 1989), cardiac muscle (Patlak and Ortiz, 1985), squid axon (Chandler and Meves, 1970; Gilly and Armstrong, 1984), and mammalian hippocampal neurons (French and Gage, 1985). Although different sensitivities to toxins of persistent versus fast-inactivating Na^+ currents have been reported (Josephson and Sperelakis, 1989; Saint et al., 1992), it is still unclear whether the two types of current are generated in the same tissue by different channel isoforms or by the same channels, which may obey different inactivation kinetics. The existence of different gating patterns of the Na^+ channel action, including different inactivation characteristics, often termed "modes," is well established (for review see Patlak, 1991). For an identification of gating modes, two main approaches have been reported up to now: 1) pharmacological intervention, which produces gating in a specific mode (e.g., Horn et al., 1984); 2) analysis of so-called "late Na^+ channel currents" (e.g., Patlak et al., 1986). In the first approach, the mode may be completely artificial. In the second approach, the contribution of channel openings in the slowly inactivating mode is low, and it cannot be proven that the late Na^+ channel currents are recorded from a Na^+ channel, which was acting in the normal mode before. In an unmodified single Na^+ channel, a detailed analysis of modal action is still lacking.

Development of a low-noise recording technique by Benndorf (1993, 1994a, b), using patch pipettes with unusually thick walls and small pores, allowed for exceptionally stable recordings from patches containing one and only one Na^+ channel. In the present study, different functional modes of a single Na^+ channel are described, which were recorded in cell-attached patches without pharmacological intervention.

MATERIALS AND METHODS

Cell preparation

Single ventricular cells were isolated by digesting hearts from adult white mice with collagenase. The procedure used here was essentially the same as described by Benndorf (1993).

Patch pipettes

The raw material for the patch pipettes was thick-walled borosilicate glass tubing (Hilgenberg, Malsfeld, Germany) with an external diameter of 2.0 mm and an internal diameter of 0.5 mm. The patch pipettes were prepared in a similar way as described by Benndorf (1994a) for the purpose of low-noise recording. In brief, the procedure consisted of three pulling steps, yielding a final pipette resistance of 40–120 MΩ when filled with double concentrated Tyrode's solution. After filling, the pipette was shortened to about 8 mm. For this purpose, it was mounted in a chuck in a clockmaker's turning lathe. The glass tube was sawn under rotation with a pin of hardened steel and finally broken in a beaker filled with filtered (0.2 μm) pipette solution. Immersion during breaking was very helpful to keep the pipette tip intact. The newly formed rear end was carefully sealed by a drop of paraffin oil. For a more detailed discussion of essential properties of thick-walled pipettes, the reader is directed to Benndorf (1994b). The short patch pipette was inserted into a pipette holder of small dimensions (Benndorf, 1993). Some experiments were performed according to the technique of Böhle and Benndorf (1994), using pipette tips generated only seconds before gigaohm seal formation. For giga-seal formation normally slight suction was applied.

Received for publication 20 June 1994 and in final form 13 October 1994.
Address reprint requests to Thomas Böhle, Department of Physiology, University of Cologne, Robert-Koch-Strasse 39, D-50931 Cologne, Germany. Tel.: 221-478-6951; Fax: 221-478-6965.
K. Benndorf is a Heisenberg fellow of the Deutsche Forschungsgemeinschaft.

0006-3495/95/01/121/10 $2.00

Solutions and temperature

The bathing solution contained (mmol/l): 230 KCl, 20 CsCl, 1 $MgCl_2$, 10 EGTA, 5 HEPES, pH 7.3. The pipette solution contained (mmol/l): 255 NaCl, 2.5 $CaCl_2$, 4 KCl, 5 HEPES, pH 7.3. The elevated Na^+ concentration was used to enhance unitary current amplitudes (Yue et al., 1989). The experiments were performed at room temperature (22–24°C).

Data acquisition and analysis

Measurements were performed on the stage of an inverted microscope. Cells were exposed to the hypertonic bath solution at least 20 min before the experiments were started. Single Na^+ channel currents were measured (band width 20 kHz, sampling interval 10 or 15 μs) in the cell-attached patch configuration with an Axopatch 200A amplifier (integrating headstage; Axon Instruments, Inc., Foster City, CA), which had an intrinsic noise of 0.068 pA rms (5 kHz). Analog filtering was performed with an 8-pole Bessel filter (48 dB/octave, Frequency Devices, Inc., Haverhill, MA). If not otherwise noted, the holding potential was −120 mV, and pulses of 4 ms duration to −40 mV were applied at a rate of 20 Hz from prepulse potentials between −180 and −70 mV (prepulse duration 20 ms). In the single-channel patches, fast Na^+ current inactivation was normally removed completely at −100 mV. Some differences of midpoint and steepness of steady-state activation and inactivation among the modes was found (Böhle and Benndorf, manuscript in preparation). Despite the high pulsing rate combined with less negative prepulse potentials, the open probability was constant. Therefore it is concluded that slow Na^+ channel inactivation was not present. This agrees with the finding that in myocardial mouse cells at −120 mV, Na^+ channels recover from slow inactivation rapidly (τ = 11 ms; Benndorf and Nilius, 1987). Capacitive transients were compensated carefully to exclude any saturation of the amplifier. To this end, the internal compensation circuit of the amplifier, which consists of two exponentials, was expanded by two further exponentials that were fed in as integral signals via the speed-test input to the headstage (Benndorf, 1993). All sweeps were corrected for leakage and remaining capacitive currents by subtracting averaged blank traces, which were formed only from traces in the neighborhood of the actual sweep. All patches were checked to see if they contained more than one active Na^+ channel by looking for any obvious superimposition of opening events in several thousands of consecutive traces (−40 mV). None of the patches in this study had any such indication. For further evaluation, data sometimes were filtered to a final cutoff frequency of 5 or 10 kHz with an off-line Gaussian filter algorithm. Histograms of the single open-channel life time were determined using the baseline method (Benndorf, 1994b). To improve resolution, amplitude histograms were formed by eliminating the transition points with the variance-mean technique (Patlak, 1988). For curve fitting, a derivative-free Levenberg-Marquardt routine (Brown and Dennis, 1972) was used. All analysis was performed with the ISO2 software (MFK Computer, Niedernhausen, Germany).

RESULTS

Variability in Na^+ current kinetics

Fig. 1 shows characteristic properties of a fast-inactivating Na^+ channel (patch 1). Pulses to −40 mV were applied from a prepulse potential of −100 mV at a frequency of 20 Hz. Openings occurred exclusively during the first 2 ms after beginning of the pulse. The ensemble-averaged current (*A*, *upper trace*) shows the typical fast time course of activation and inactivation. The histogram of the open-channel life time (*B*) was formed by making use of the baseline method (Benndorf, 1994b). A reasonable fit was possible with a single exponential yielding the time constant τ_o of 0.16 ms. The cumulative first-latency distribution (*C*) reveals that openings appeared in 46% of the traces. The time ($t_{0.5}$) before which half of the first channel openings had occurred, referred only to traces with openings, was 0.18 ms.

Fig. 2 illustrates the ensemble-averaged current of 1002 traces formed from the unitary currents in a slowly inactivating Na^+ channel. The patch (patch 2) was stable for 1.5 h and current kinetics was slow from the beginning to the end

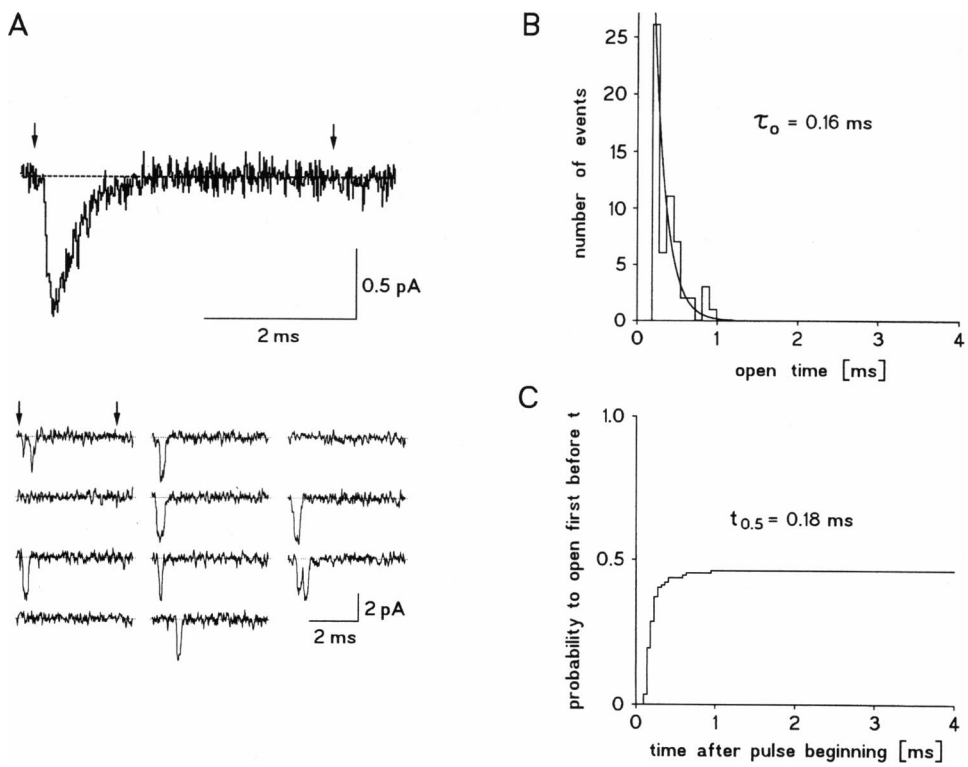

FIGURE 1 Typically fast-inactivating Na^+ currents obtained from a patch with one and only one channel (patch 1; pipette resistance 17 MΩ; seal resistance 27 GΩ; prepulse potential −100 mV; test pulses to −40 mV; filter 20 kHz). (*A*) Ensemble-averaged current formed from 119 sweeps (top; filter 20 kHz). Eleven selected traces (bottom; filter 5 kHz). The arrows indicate beginning and end of the test pulses. (*B*) Histogram of the open-channel life time. The data could be fitted monoexponentially (119 traces; filter 10 kHz; baseline method; binwidth 90 μs). (*C*) Cumulative first-latency distribution. The probability of traces with one or more openings was 46%. The time before which half of the first channel openings had occurred ($t_{0.5}$; referred only to traces with openings) was 0.18 ms (119 traces; filter 5 kHz; threshold 50%; binwidth 45 μs).

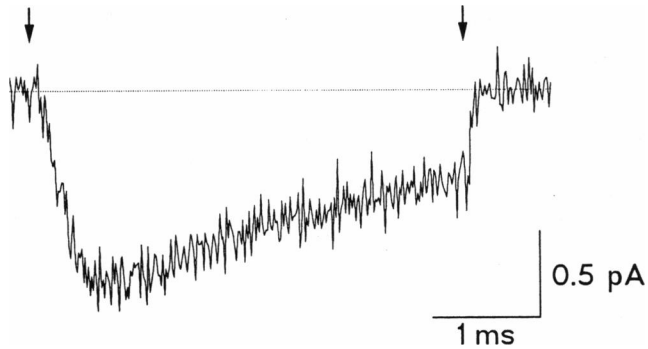

FIGURE 2 Ensemble-averaged current formed from 1002 traces of a patch containing one and only one Na^+ channel with slow inactivation characteristics. The arrows indicate beginning and end of the test pulses (patch 2; pipette resistance 97 MΩ; seal resistance 1000 GΩ; prepulse potential −180 mV; test pulses to −40 mV; filter 20 kHz).

of the experiment. Pulses of 4 ms duration were applied to −40 mV from a prepulse potential of −180 mV. Since other prepulse potentials had no effect on the kinetics of this current, the more negative prepulse potential compared to that in Fig. 1 is without significance for inactivation kinetics. Inactivation was incomplete after 4 ms of depolarization. The time-to-peak was longer compared with that of the ensemble-averaged current in Fig. 1. Thus, activation was slowed in parallel to inactivation.

Fig. 3 illustrates an experiment in which one Na^+ channel (patch 3) dramatically changed its kinetics within 0.5 h. The traces in *A* present the ensemble-averaged currents recorded at different times of the experiment. At the beginning (1), complete inactivation of the ensemble-averaged current was reached during the pulse of 4 ms duration, although inactivation was not as fast as in Fig. 1 *A*. After 15 min (4), inactivation was incomplete having a time course, similar to that observed in Fig. 2. After 23 min (6), partial inactivation was followed by a second peak. Concomitantly with the increasing inactivation deficit, the amplitude of the ensemble-averaged current decreased. The right hand plots in *A* illustrate the long-time courses of the averaged current per trace. Each point represents the averaged current of an individual sweep of 4 ms duration. For the long-time course, averaged currents per trace were used because of heterogeneities in amplitude (Benndorf, 1993), which severely complicate evaluation of the open probability. The plots indicate that alterations in single-channel characteristics must have happened. While the points became distributed more evenly during transition from (1) to (4), they concentrated at lower levels during transition from (4) to (7). In *B*, the ensemble-averaged currents (1, 3, 4) were scaled with respect to the maximum to demonstrate that also the time-to-peak was prolonged.

To exclude a slow voltage shift during the experiment to more negative potentials because of some change in the actual concentration of Na^+ ions on either side of the membrane, which could also explain these observations, amplitude histograms were formed during the progress of the

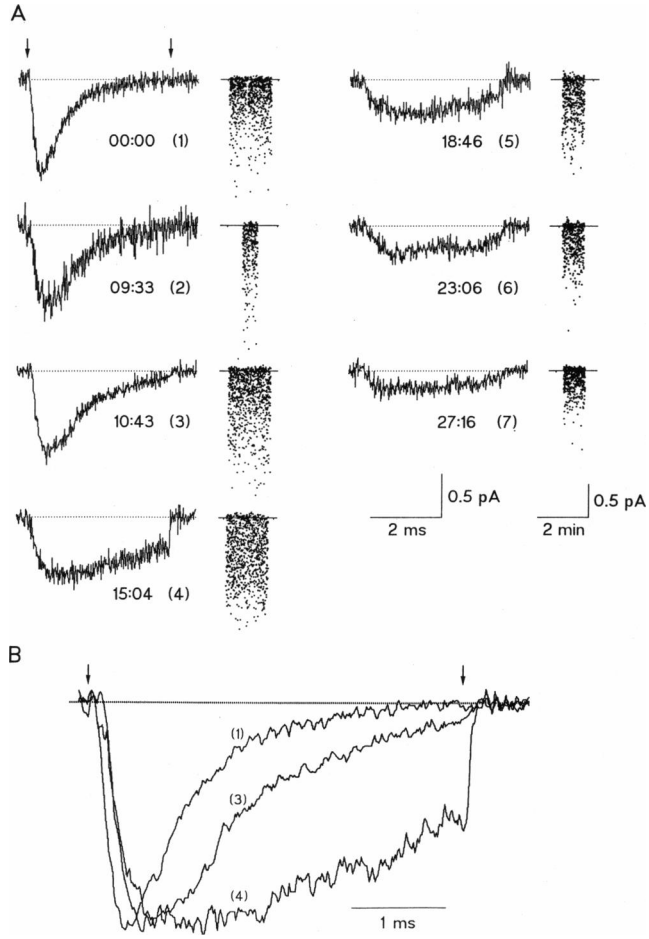

FIGURE 3 Continuous transition from rather fast to slow Na^+ current inactivation during a time interval of 27 min in a patch with one and only one channel. The arrows indicate beginning and end of the test pulses (patch 3; pipette resistance 42 MΩ; seal resistance 800 GΩ; prepulse potential −150 mV (1), −180 mV (2), (3), (5), (6), (7), −120 mV (4); test pulses to −40 mV; filter 20 kHz). (*A*) Ensemble-averaged currents (*traces, left*) and long-time courses of the averaged current per trace (*dots, right*), arranged according to the progress (1–7) of the experiment. Every dot represents the averaged current of an individual trace of 4 ms duration (1002 traces (1), 363 traces (2), 1006 traces (3), 1001 traces (4), 510 traces (5), 501 traces (6), 501 traces (7); filter 20 kHz). (*B*) Currents (1), (3), (4) normalized with respect to the peak amplitude (filter 5 kHz).

experiment in patch 3. With a single-channel conductance of 25 pS, a change in the driving force of −40 mV would have produced a change in the single-channel current amplitude of −1 pA. In Fig. 4, the time in the experiment is indicated below each amplitude histogram. The numbers in brackets correspond to those in Fig. 3. A Gaussian function could be fitted to the open-level distribution in all cases. The mean single-channel current was constant during the whole experiment. Thus, a change in the electrochemical driving force across the pore of the channel can be excluded.

In the following, the mechanisms underlying the changes in current kinetics in patch 3 are analyzed in more detail. In the left diagram of Fig. 5 *A*, a histogram of the open-channel life time is shown, which was built from 1001 traces corresponding to (1) in Fig. 3. Here, with inactivation being

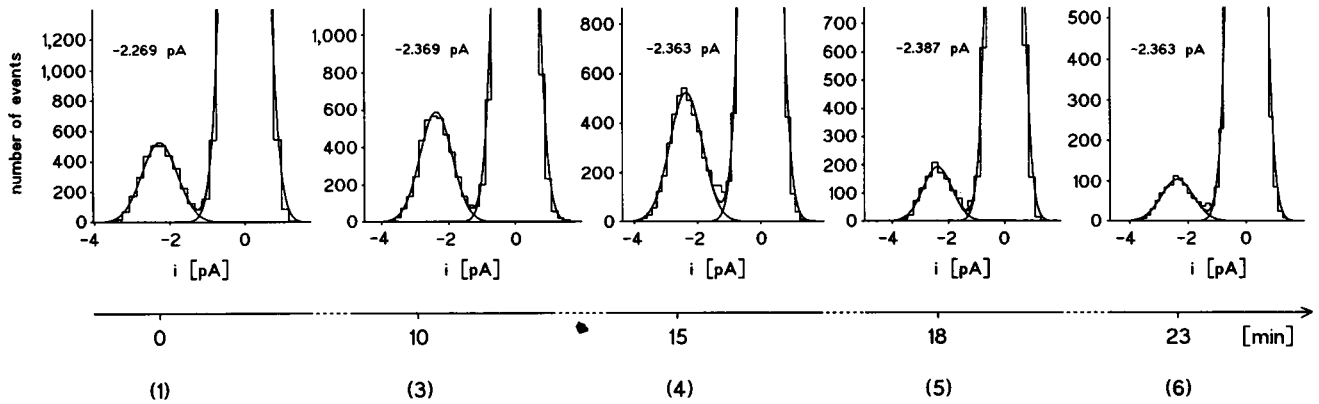

FIGURE 4 Absence of a change in the electrochemical driving force during alterations in current kinetics in patch 3. Five amplitude histograms from traces recorded at the indicated times after beginning of the experiment are presented. The numbers in brackets correspond to those in Fig. 3. The distributions were fitted with two Gaussian curves. The peak of the baseline noise is truncated. The mean open-channel currents are indicated. The constancy of the mean single channel Na^+ current amplitude reveals that the electrochemical driving force across the channel pore did not change (filter 20 kHz; window width for variance-mean analysis 75 μs; threshold variance 0.2 pA^2).

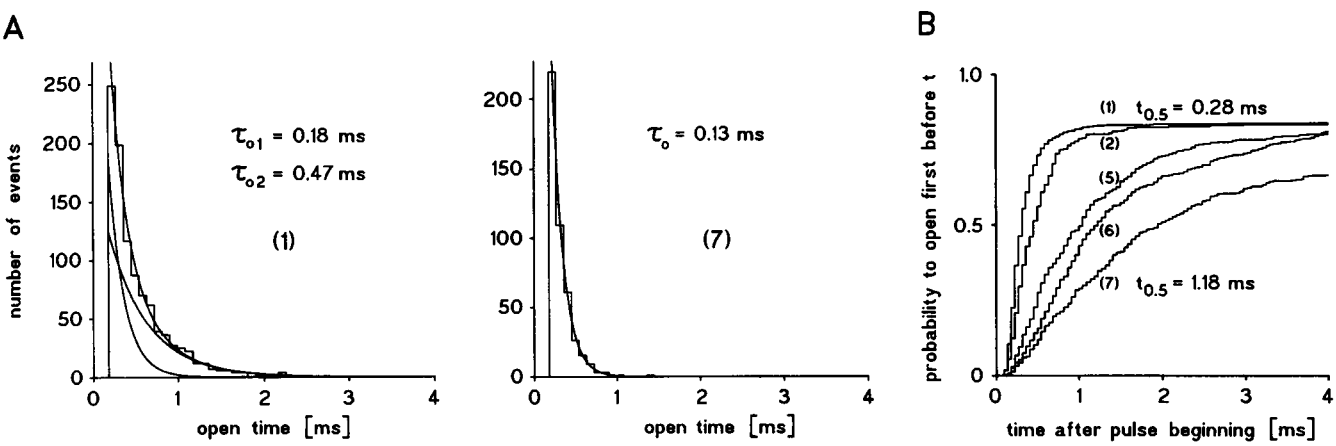

FIGURE 5 Alterations in the mean open time and first latency underlying the changes in current kinetics in patch 3. (*A*) Histograms of the open-channel life time corresponding to (1) and (7) in Fig. 3. At the beginning, two exponentials were present, whereas only a short exponential was present at the end of the experiment (filter 10 kHz; baseline method; binwidth 90 μs). (*B*) Cumulative first-latency distributions corresponding to (1), (2), (5), (6), (7) in Fig. 3. The probability of traces with one or more openings was reduced from 84.5% (1) to 67.5% (7). The time before which half of the first channel openings had occurred ($t_{0.5}$; referred only to traces with openings) was prolonged from 0.28 ms (1) to 1.18 ms (7); (filter 10 kHz; threshold 60%; binwidth 45 μs).

complete after 4 ms, two different mean open times (τ_{o1} = 0.18 ms; τ_{o2} = 0.47 ms) were present. It might be expected that the slowly inactivating ensemble-averaged currents were caused by openings matching predominantly the slow time constant. The right open-time histogram corresponds to (7) in Fig. 3 when inactivation was nearly absent. Surprisingly, here only a fast (τ_o = 0.13 ms) time constant was present. This clearly indicates that another mechanism must be responsible for the altered inactivation kinetics. The mean open times for the other traces were 0.32 ms (2), 0.35 ms (3), 0.25 ms (4), 0.13 ms/0.25 ms (5), 0.16 ms (6). In Fig. 5 *B*, cumulative first-latency distributions at the respective stages of the experiment are shown. The probability to record traces with channel activity decreased from 84.5% (1) to 67.5% (7). The time before which half of first channel openings had occurred ($t_{0.5}$) increased from 0.28 ms (1) to 1.18 ms at the end of the experiment (7). Thus, the increasing inactivation-deficit finds an explanation in the prolongation of the first latency.

Identification of modes of Na^+ channel action

Besides slow alterations in Na^+ channel action, fast and repetitive switches between different modes of Na^+ channel gating were observed. In Fig. 6 such switches are demonstrated by the plot of the long-time course of the averaged current per trace. Again (see also Fig. 3), each point represents the averaged current of an individual sweep of 4 ms duration. Different modes may be easily identified by the different plateau-like patterns formed by points. Records from three different patches (*A:* patch 4, *B:* patch 3, *C:* patch 2) are shown, in which the life-time of individual modes was

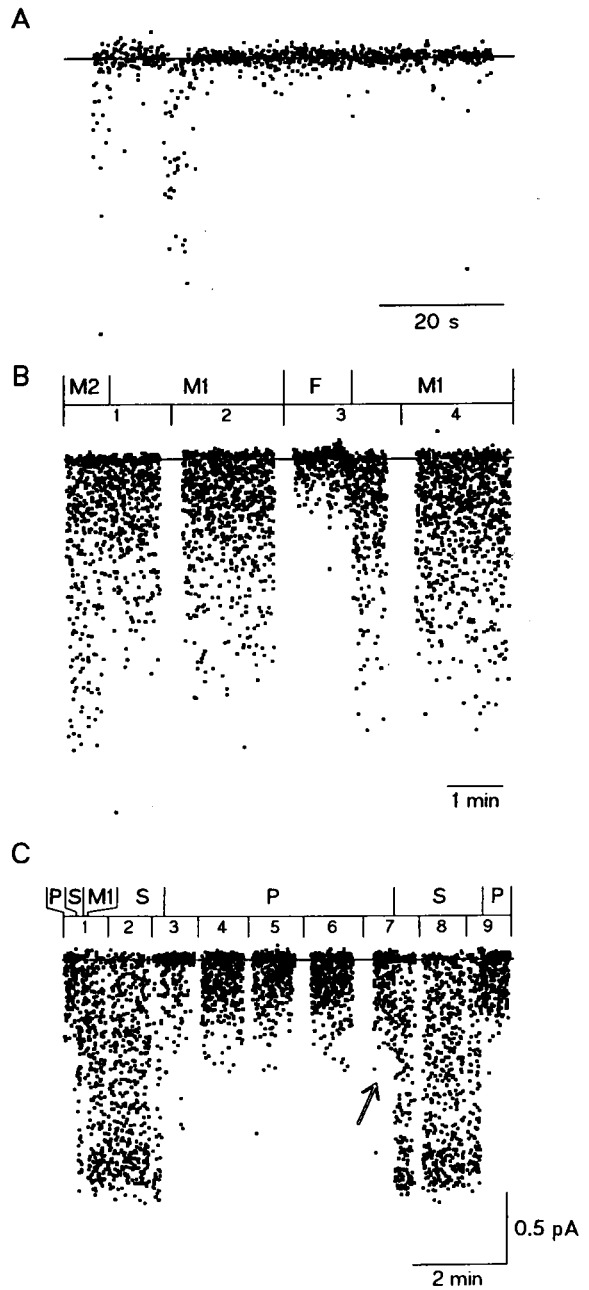

FIGURE 6 Fast and repetitive switches between different modes of Na^+ channel action, identified by plots of the long-time course of the averaged current per trace in 3 different patches (*A, B, C;* different time scales; filter 20 kHz). The switches were independent of different prepulse potentials. Every dot represents the averaged current of an individual sweep of 4 ms duration. Intervals without points in (*B*) and (*C*) correspond to pauses in pulsing and recording. (*A*) Different modes in one block of continuous recording (patch 4; 992 traces; pipette resistance 55 MΩ; seal resistance 100 GΩ; holding potential −190 mV; no prepulses; test pulses to −50 mV). (*B*) Three different modes (M2, M1, F) in four numbered blocks of continuous recording each (patch 3; 4005 traces; prepulse potential −90 mV (block 1), −120 mV (block 2), −180 mV (blocks 3 and 4); test pulses to −40 mV). (*C*) Three different modes (P, S, M1) in 9 numbered blocks of continuous recording each (patch 2; 4551 traces; prepulse potential −180 mV (block 1), −170 mV (block 2), −160 mV (block 4), −140 mV (block 6), −130 mV (block 8), −110 mV (block 9), −100 mV (block 7), −80 mV (block 5), −70 mV (block 3); test pulses to −40 mV). The open arrow points on a mode switch that had arisen within a block of continuous recording (block 7).

dramatically different. Short intercepts without points in *B* and *C* indicate pauses in pulsing and recording.

In Fig. 6 *A* (patch 4), one block of continuous recording is illustrated, in which only two short intervals of about 5 s each with switches to modes characterized by enhanced averaged current per trace are visible.

In Fig. 6 *B* (patch 3), four numbered blocks of continuous recording each are shown. Here, different modes lasted for longer times in the range of 1–2.5 min. The switches were independent of different prepulse potentials (see legend). Three different levels may be detected easily. The channel switched from a large (M2) to an intermediate (M1), then to a small (F), and again to the intermediate level. The abbreviations (M2, M1, F) written on top of the blocks are inserted for identification of the different modes and are further explained in Table 1 in Discussion. This applies also to the following figures. In Fig. 6 *B*, block 3 (only the part with M1 mode) and block 4 are identical with the plots (2) and (3) in Fig. 3 *A*, respectively. Besides the switches shown in Fig. 6 *B*, no further mode switches were obvious in the experiment, but the maximum level of the averaged current per trace (the plateau) progressively declined, as shown in Fig. 3. Thus in patch 3, both M2 mode and F mode was detected only once, and M1 mode twice.

In the patch of Fig. 6 *C* (patch 2), three different modes were present. Only part of the experiment, with nine numbered blocks of continuous recording each, is shown. In the whole experiment, the P mode appeared for up to 10 min and in summary four times. The S mode lasted for up to 8 min and was observed six times. The M1 mode was detected only twice for short time intervals in the range of some seconds. One occurrence of M1 mode of 4 s duration is illustrated at the left of this plot. In summary, M1 mode appeared for only about 1% of the whole time, while P- and S mode were each present for nearly 50% of the time. In the whole experiment, different prepulse potentials between −60 mV and −180 mV were applied, which however had no effect on the switching between different modes. This is concluded from the fact, that within blocks of continuous recording, switching from P- to S mode happened when prepulse potentials were either −180 mV (block 1) or −100 mV (block 7) and in the opposite direction (from S- to P mode) when prepulse potentials were −110 mV (block 9) or -70 mV (block 3). In parts of the experiment not shown in Fig. 6 *C*, S mode was constant for about 500 traces with prepulses of −180 mV and −60 mV and P mode with prepulses of −180 mV and −90 mV. In one block of continuous recording at −180 mV (block 1), all three modes present in this patch were observed, i.e. switching from P- to S to M1 and again to S mode happened. So it is concluded, that no dependence on the prepulse potential existed and that the switching appeared at random.

A change of surface charge would alter the field in the immediate vicinity of the channel, thereby possibly affecting the voltage sensitivity of gating, but not necessarily the single

channel conductance. Such alterations in surface charge cannot be excluded by the kind of test as applied in Fig. 4. The switching in Fig. 6 provides an argument against a slow change of the voltage seen by the voltage sensor or some other slow continuous change in the patch during recording, since the modal changes took place both back and forth.

The switching itself was instantaneous in all patches, i.e. a transition-time course could not be resolved. The open arrow in Fig. 6 *C* marks a mode switch, that had happened within a block of continuous recording. In Fig. 7 (patch 2), 22 traces in the direct neighborhood of this mode switch are plotted. Out of the eleven traces directly before the switch (left; P mode), five traces were without openings. The remaining six traces had openings appearing not very closely correlated to the beginning of the pulse. Hgeterogenous levels in Na^+ current amplitude (see Benndorf, 1993) were present. In the eleven traces recorded directly after the switch (right; S mode), only one was without opening. In the other ten traces, the openings started promptly after pulse beginning and lasted in part nearly for the whole pulse duration. Here heterogenous amplitudes were rare.

Ensemble-averaged currents from different modes are illustrated in Fig. 8. In panel A, they were obtained from the traces before and after the mode switch in block 3 of Fig. 6 *B* (patch 3). The F mode had a fast, whereas the M1 mode had an intermediate inactivation kinetics. In panel B, the left current was formed from 156 traces of the S mode in patch 2. Here inactivation was incomplete after 4 ms and a small tail current related to deactivation was resolved. During the whole experiment, this kinetics was typical always when the S mode was present. The right current in *B* was formed from 350 traces and obtained from the same block of continuous recording as the left, but after having switched to the P mode. This current had a small amplitude and was deficient of any inactivation. This kinetics was typical always when the P mode was present. It looked similar to that obtained in trace (7) of Fig. 3 (patch 3). These two currents are compared further in Table 1 in Discussion.

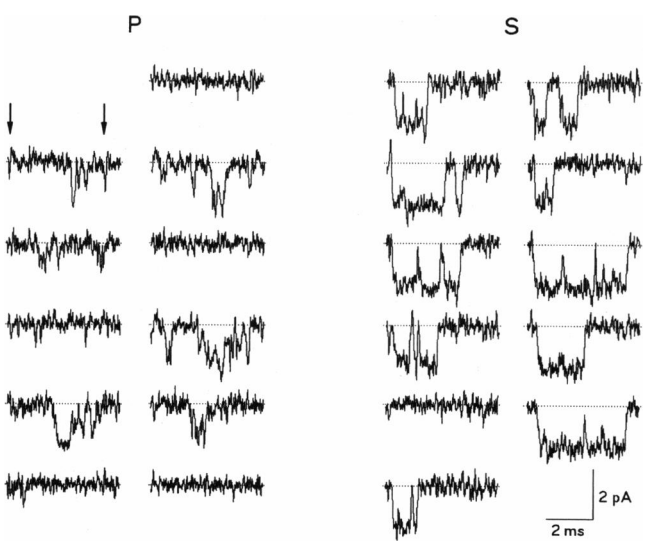

FIGURE 7 Eleven current traces directly before (left; P mode) or after (right; S mode) the switch in block 7 marked by the open arrow in Fig. 6 *C*. The arrows indicate beginning and end of the test pulses (patch 2; prepulse potential −100 mV; test pulses to −40 mV; filter 5 kHz).

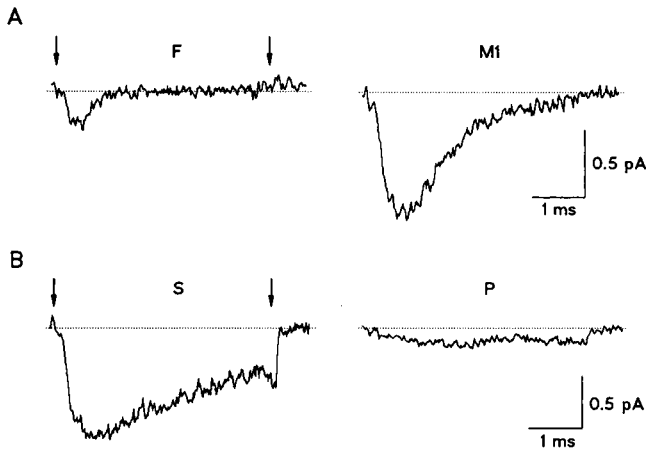

FIGURE 8 Ensemble-averaged currents formed from different modes before and after a switch. The arrows indicate beginning and end of the test pulses. (*A*) Mean currents from F mode (640 traces) or M1 mode (363 traces), respectively, of block 3 in Fig. 6 *B* (patch 3; prepulse potential −180 mV; test pulses to −40 mV; filter 5 kHz). (*B*) Mean currents from S mode (156 traces) or P mode (350 traces), respectively, of block 9 in Fig. 6 *C* (patch 2; prepulse potential −110 mV; test pulses to −40 mV; filter 5 kHz).

The mechanisms underlying the kinetic changes of the averaged currents were analyzed in Fig. 9. Part *A* illustrates the open-time distribution of the S mode and the P mode in patch 2. In the S mode, two open times were found. One was long (τ_{o2} = 1.01 ms), while the other was short (τ_{o1} = 0.13 ms). To increase the quality of the open-time histogram in the P mode, it was built from 1526 traces of three successive blocks of continuous recording each. The P mode was dominated by a short time constant only (τ_o = 0.13 ms). A typical cumulative first-latency distribution for the P mode is illustrated by the lower curve in *B*. Its time course was slow, yielding the time before which half of the first channel openings had occurred ($t_{0.5}$) of 1.17 ms. The S mode showed a much faster first latency with $t_{0.5}$ of 0.26 ms and a significantly higher probability of non-empty traces (81%) than the P mode (51%).

Although in some cases the occurrence of heterogenous levels in single channel Na^+ current amplitude was different before and after mode switches, amplitude histograms showed that the mean single-channel conductance was not altered by mode switches. In Fig. 10, amplitude histograms were formed from the M2 mode or the M1 mode, respectively, of the first block in Fig. 6 *B* (patch 3). The mean single-channel currents at pulses to −40 mV were practically identical, being 2.351 pA in the M2 mode and 2.358 pA in the M1 mode.

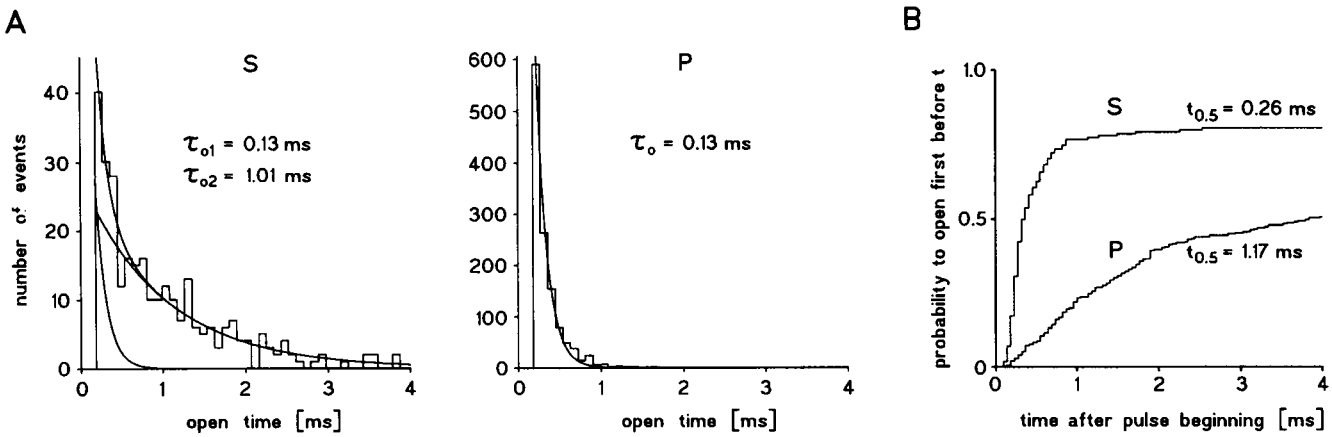

FIGURE 9 Alterations in the mean open time and first-latency distribution by mode switches. (*A*) Typical histograms of the open-channel life time of S mode (248 traces; block 7 in Fig. 6 *C;* prepulse potential −100 mV) and P mode (1526 traces in three successive blocks of continuous recording each; prepulse potentials −180 mV, −120 mV, or −150 mV, respectively). The data could be fitted monoexponentially for P mode and biexponentially for S mode (patch 2; test pulses to −40 mV; filter 10 kHz; baseline method; binwidth 90 μs). (*B*) Cumulative first-latency distributions of S mode (upper curve; 156 traces) or P mode (lower curve; 350 traces) in Fig. 6 *C* (block 9; prepulse potential −110 mV; test pulses to −40 mV). The probability of non-empty traces was reduced from 81% to 51%. The time before which half of the first channel openings had occurred ($t_{0.5}$; referred only to traces with openings), was prolonged from 0.26 ms to 1.17 ms (patch 2; filter 5 kHz; threshold 66%; binwidth 45 μs).

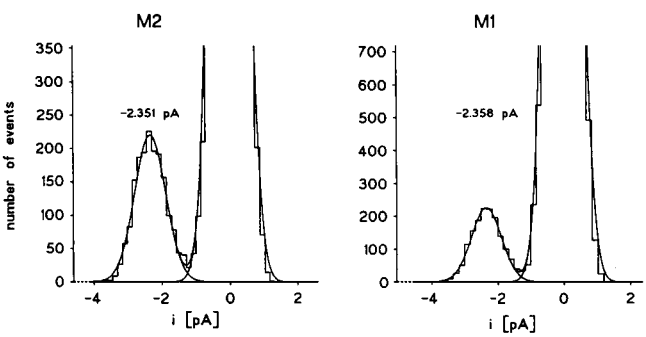

FIGURE 10 Mode switches do not alter the single channel conductance. Amplitude histograms formed from openings in M2 mode (400 traces) or M1 mode (601 traces) of block 1 in Fig. 6 *B*. The distributions were fitted with two Gaussian curves. The peak of the baseline noise is truncated. The mean open-channel currents are indicated (patch 3; filter 20 kHz; prepulse potential −90 mV; test pulses to −40 mV; window width for variance-mean analysis 75 μs; threshold variance 0.2 pA^2).

DISCUSSION

Gating in a Na^+ channel is multimodal

In this paper, mode switches of cardiac Na^+ channels were studied in extraordinarily small patches containing one and only one channel. The different modes were identified in the averaged current per trace plotted over long times by direct switching between two of them. Specific for the modes were: 1) the distribution of the open-channel life time and 2) the distribution of the first latency. These characteristic properties generated ensemble-averaged currents differing in kinetics and amplitude. It shall be stressed here that most of the data included in evaluation correspond to channels, which inactivated with unusually slow kinetics. In Table 1, all modes observed in Fig. 6, *B* and *C*, are ordered with respect to the increasing inactivation deficit inherent in the ensemble-averaged currents. The final ensemble-averaged

TABLE 1 Different modes of Na^+ channel action

Name of mode	Example	First latency ($t_{0.5}$)	Mean open time (τ_0)	Probability of non-empty traces	Amplitude of ensemble-averaged current	Inactivation kinetics
Fast-inactivating (F)		Fast	Short	Low	Variable	Fast
	Fig.6B (block 3; patch 3)	0.25 ms	0.15 ms	36 %	0.23 pA	
	Fig. 1 (patch 1)	0.18 ms	0.16 ms	46 %	0.95 pA	
Intermediate 1(M1)		Fast	Intermediate	Intermediate	Intermediate	Fast–intermediate
	Fig. 6B (patch 3)	0.28 ms	0.31 ms	68 %	0.84 pA	
Intermediate 2 (M2)		Fast	Intermediate	Intermediate	Large	Intermediate–slow
	Fig. 6B (block 1; patch 3)	0.25 ms	0.42 ms	72 %	1.05 pA	
Slow (S)		Fast	Long	High	Large	Slow
	Fig. 6C (patch 2)	(0.26 ms)	1.01 ms/(0.13 ms)	(81 %)	(1.04 pA)	
Persistent (P)		Slow	Short	Intermediate	Small	Absent
	Fig. 6C (patch 2)	1.17 ms	0.13 ms	51 %	0.15 pA	
	Fig. 3 (trace 7; patch 3)	1.18 ms	0.13 ms	67.5 %	0.28 pA	

current in the patch with the slow and time-dependent changes (patch 3; trace (7) in Fig. 3) was included, since it had a nearly complete identity with the P mode in patch 2. We are aware that the names attributed to the individual modes are somehow arbitrary, but we decided to introduce them to facilitate further discussion. All parameters in Table 1 correspond to a test-pulse potential of −40 mV.

The F mode (fast-inactivating) is characterized by a short mean open-channel life time, a fast first latency, and a relative low probability of non-empty sweeps. In the experiment illustrated in Fig. 1, the Na^+ channel only gated in the F mode. In Fig. 6 *B*, the F mode occurred for a short interval of about 1 min. Before and after, a mode called M1 was present. Both the M1- and M2 mode are intermediate types with respect to kinetics of macroscopic inactivation. They are characterized by an intermediate mean open-channel life time, a fast first latency, and an intermediate probability of non-empty sweeps. Although their single channel characteristics differ only slightly, they are distinguished here, because of the clear switch from M2 to M1 illustrated in Fig. 6 *B*. The S mode (slowly inactivating) is characterized by a fast first latency and high probability to obtain traces with openings. Two different mean open-channel life times were measured, a long and a short. A repetitive switching to the persistent (P) mode was observed, which had one mean open time of short duration. From this, it is suggested, that in the S mode a small portion of P mode was hidden, causing the second (slow) mean open-time constant, which is therefore covered in brackets in the table. If this is correct, then in the S mode the true probability of non-empty sweeps is larger than 81%, $t_{0.5}$ is faster than 0.26 ms, and the amplitude of the ensemble-averaged current is larger than 1.04 pA. Hence, the mean open time of the S mode is about 1 ms. It might even be longer, since some openings were probably truncated by repolarization. The P mode (persistent) is characterized by a short mean open-channel life time, a slow first latency, and an intermediate probability of non-empty sweeps. In summary, the following switches were identified: 1) F to M1 mode, 2) M1 to F mode, 3) M2 to M1 mode, 4) M1 to S mode, 5) S to M1 mode, 6) S to P mode, and 7) P to S mode. The transitions between modes imply at least two types of modulation in the gating behavior: 1) The observed alterations in the first-latency distribution indicate altered activation gating. 2) Shortening of the mean open time concomitantly with the loss of inactivation in the ensemble-averaged current reveals that also deactivation was affected.

Is the slow loss of inactivation based on a continuous mode alteration?

Our way of identification of different modes included in Table 1 is based on abrupt switching from one mode to another. The continuous transition between different types of inactivation illustrated in Fig. 3 *A* (patch 3) is discussed here. Since in nearly all its properties (Table 1), current (7) in Fig. 3 was identical to the P mode, it is concluded that in this experiment the P mode was present at the end. The two different mean open times inherent in traces (1) and (5) suggest that both were composed of two different modes each. From Figs. 3 and 6 and from Table 1, it can be derived that traces (2) and (3) in Fig. 3 represent the M1 mode. Only one individual mean open time was also present in traces (4) and (6) in Fig. 3. If these traces correspond to single modes each, then more modes than shown in Table 1 may exist. If they were composed of the modes described in Table 1, it might be that these were not resolved, because their mean open times differed only by little and their life times were only short. In favor of this idea is 1) the observed short life times of the modes shown in Fig. 6 *A* and 2) the bimodal open-time distribution inherent in the S mode and also in traces (1) and (5) of Fig. 3. Hence, the slow transition from rather fast to slow inactivation may have been caused by a slow alteration in the ratio of modes and/or by a slow mode shift.

Comparison with previous results

In frog skeletal muscle, Patlak et al. (1986) observed a "bursting mode," which seems to be different from the modes as detected herein, because very long-lasting Na^+ channel openings were correlated with complete absence of inactivation. The mean open times varied from burst to burst and also significant heterogeneity was seen within 20% of individual bursts. Since the bursts were identified as "late Na^+ channel currents" in multichannel patches, the authors could not decide, whether both the transition to the bursting mode and the open-time heterogeneity within and between different bursts was an expression of different subpopulations of channels or was based on a mode shift of a single channel. In the present report we are sure that we observed different gating modes, because in each patch one and only one Na^+ channel was active.

The spontaneous appearance of both abrupt switches and slow alterations of macroscopic inactivation in a single Na^+ channel complicates any classification into fast-inactivating and non-inactivating types of Na^+ channels. Differences in the sensitivity of persistent versus fast-inactivating Na^+ currents to pharmacological probes (e.g., Saint et al., 1992) are also not convincing to prove the existence of two different Na^+ channel populations, because one can assume that the sensitivity of channel proteins to drugs varies with the channel's configuration (Hille, 1977): a mode with a high open probability should bind a drug, which has a higher affinity to the open configuration, more effectively, than does a mode with a low open probability. Hence, modes also would have different pharmacological sensitivities. The existence of distinct Na^+ channel populations differing in macroscopic inactivation kinetics may therefore only be proven, if it is directly shown, that different Na^+ channel isoforms (Cohen and Barchi, 1992) are involved.

Possible reasons for multimodal action of Na^+ channels

Among other possibilities, the observed multimodal gating of Na^+ channels might be caused by 1) phosphorylation pro-

cesses (Sunami et al., 1991; Numann et al., 1991) or 2) mechanisms involving intracellular Ca^{2+} (Egger and Greef, 1994), cytoskeleton (Cantiello et al., 1991), and/or mechanical actions on plasma membrane (Böhle and Benndorf, 1994).

Functional modulation of cardiac and brain Na^+ channels by phosphorylation has been investigated by several groups (Sunami et al., 1991; Sorbera and Morad, 1991; Ono et al., 1993; Numann et al., 1991; West et al., 1991; Li et al., 1993; Godoy and Cukierman, 1994). In rat brain Na^+ channels, five distinct cAMP-dependent protein kinase phosphorylation sites and one protein kinase C (PKC) phosphorylation site were identified. The target site for PKC phosphorylation is a serine residue (serine 1506) in the intracellular loop between homologous domains III and IV of the α-subunit of the Na^+ channel. It seems to be directly coupled to inactivation mechanisms of the channel. When 1-oleoyl-2-acetyl-*sn*-glycerol (OAG), a specific activator of PKC, was added, two effects were observed: 1) the peak Na^+ current decreased by up to 80%; 2) the inactivation of Na^+ channels was slowed. Since no activators or inhibitors of PKC were used in the present study, mode switches might have been triggered by the spontaneous action of PKC.

As a further regulatory mechanism for the Na^+ channel, Egger and Greef (1994) showed a crosstalk between the intracellular Ca^{2+} concentration and phosphorylation in N1E115 neuroblastoma cells. Work on Na^+ channels in frog skeletal muscle (Stühmer and Almers, 1982) and renal epithelium (Cantiello et al., 1991) suggests that cytoskeletal components also regulate channel function. Influences of both cytoskeleton and membrane bending on the channel action may result from suction applied to the patch under experimental conditions (Sokabe et al., 1991). In a previous report we showed (Böhle and Benndorf, 1994) that in cell-attached patches of most likely planar configuration, which were obtained by giga-seal formation under zero pressure, Na^+ channel activity is seven times higher than in suction-induced cell-attached patches. We believe that suction in patch-clamp experiments, however, need not be ultimately unphysiological, because in a beating heart cell, the tension of both the cytoskeleton and the plasma membrane varies in a cyclic manner. Also bending of the plasma membrane occurs along with every contraction-relaxation cycle. Thus, contraction itself might be a trigger for the synchronous appearance of modes in cardiac Na^+ channels.

Four different types of Na^+ current have been identified in single beating cells of chick embryo heart and have been correlated to different phases of the action potential by direct measurement (Liu et al., 1992; Mazzanti and DeFelice, 1987;Wellis et al., 1990). These were the 1) normal fast-inactivating Na^+ current during the upstroke of the action potential; 2) outward Na^+ current after the upstroke lasting for 30 to 40 ms; 3) rare brief isolated; and 4) rare long-lasting Na^+ current events, which both last throughout the action potential plateau. The authors of the cited papers favor the possibility that the three different types of late Na^+ currents flow through the same channels that carry the fast-inactivating Na^+ current. If these are different modes of Na^+ channel action, they might be triggered by the actual contraction status of the beating heart cell. In this respect, the Na^+ channel would be physiologically regulated by some type of mechano-sensitivity. For the Ca^{2+} channel, in which also modal gating has been shown (Pietrobon and Hess, 1990), Johnson and Byerly (1993) recently reported a cytoskeletal mechanism for metabolic dependence and inactivation by intracellular Ca^{2+}. Hence, modal action of a channel molecule might be the result of an interaction of different factors as metabolism, intracellular Ca^{2+}, cytoskeleton, and plasma membrane.

We thank D. Metzler and R. Kemkes for excellent technical assistance and B. Doepner for carefully reading the manuscript.

REFERENCES

Benndorf, K. 1993. Multiple levels of native cardiac Na^+ channels at elevated temperature measured with high-bandwidth/low-noise patch clamp. *Pflügers Arch.* 422:506–515.

Benndorf, K. 1994a. Properties of single cardiac Na channels at 35°C. *J. Gen. Physiol.* In press.

Benndorf, K. 1994b. Low noise recording. *In* Single Channel Recording, 2nd ed. B. Sakmann and E. Neher, editors. Plenum Publishing Corp., New York. In press.

Benndorf, K., and B. Nilius. 1987. Inactivation of sodium channels in myocardial mouse cells. *Eur. Biophys. J.* 15:117–127.

Böhle, T., and K. Benndorf. 1994. Facilitated giga-seal formation with a just originated glass surface. *Pflügers Arch.* 427:487–491.

Brown, K. M., and J. E. Dennis Jr. 1972. Derivative-free analogues of the Levenberg-Marquardt and Gauss algorithms for nonlinear least squares approximation. *Num. Math.* 18:289–297.

Cantiello, H. F., J. L. Stow, A. G. Prat, and D. A. Ausiello. 1991. Actin filaments regulate epithelial Na^+ channel activity. *Am. J. Physiol.* 261: C882–C886.

Chandler, W. K., and H. Meves. 1970. Evidence for two types of sodium conductances in axons perfused with sodium fluoride solution. *J. Physiol. (Lond.).* 211:653–678.

Cohen, S. A., and R. L. Barchi. 1992. Cardiac sodium channel structure and function. *Trends Cardiovasc. Med.* 2:133–140.

Egger, M., and N. G. Greef. 1994. Modulation of the number of activatable Na^+ channels by $[Ca^{2+}]_i$ and a phosphatase blocker. *Biophys. J.* 66:203a (Abstr.).

French, C. R., and P. W. Gage. 1985. A threshold sodium current in pyramidal cells in rat hippocampus. *Neurosci. Lett.* 56:289–293.

Gage, P. W., G. D. Lamb, and B. T. Wakefield. 1989. Transient and persistent sodium currents in normal and denervated mammalian skeletal muscle. *J. Physiol. (Lond.).* 418:427–439.

Gilly, W. M. F., and C. M. Armstrong. 1984. Threshold channels—a novel type of sodium channel in squid giant axon. *Nature (Lond.).* 309:448–450.

Godoy, C. M. G., and S. Cukierman. 1994. Multiple effects of protein kinase C activators on Na^+ currents. *Biophys. J.* 66:202a (Abstr.).

Hille, B. 1977. Local anesthetics: Hydrophilic and hydrophobic pathways for the drug-receptor reaction. *J. Gen. Physiol.* 69:497–515.

Hodgkin, A. L., and A. F. Huxley. 1952. The dual effect of membrane potential on sodium conductance in the giant axon of Loligo. *J. Physiol. (Lond.).* 116:497–506.

Horn, R., C. A. Vandenberg, and K. Lange. 1984. Statistical analysis of single sodium channels. Effects of *N*-bromoacetamide. *Biophys. J.* 45: 323–335.

Johnson, B. D., and L. Byerly. 1993. A cytoskeletal mechanism for Ca^{2+} channel metabolic dependence and inactivation by intracellular Ca^{2+}. *Neuron.* 10:797–804.

Josephson, I. R., and N. Sperelakis. 1989. Tetrodotoxin differentially blocks peak and steady-state sodium channel currents in early embryonic chick

ventricular myocytes. *Pflügers Arch.* 414:354–359.

Li, M., J. W. West, R. Numann, B. J. Murphy, T. Scheuer, and W. A. Catterall. 1993. Convergent regulation of Na^+ channels by protein kinase C and cAMP-dependent protein kinase. *Science.* 261: 1439–1442.

Liu, Y., L. J. DeFelice, and M. Mazzanti. 1992. Na channels that remain open throughout the cardiac action potential plateau. *Biophys. J.* 63: 654–662.

Mazzanti, M., and L. J. DeFelice. 1987. Na channel kinetics during the spontaneous heart beat in chick ventricle cells. *Biophys. J.* 52: 95–100.

Numann, R., W. A. Catterall, and T. Scheuer. 1991. Functional modulation of brain sodium channels by protein kinase C phosphorylation. *Science.* 254:115–118.

Ono, K., H. A. Fozzard, and D. A. Hanck. 1993. Mechanism of cAMP-dependent modulation of cardiac sodium channel current kinetics. *Circ. Res.* 72:807–815.

Patlak, J. B. 1988. Sodium channel subconductance levels measured with a new variance-mean analysis. *J. Gen. Physiol.* 92:413–430.

Patlak, J. B. 1991. Molecular kinetics of voltage-dependent Na^+ channels. *Physiol. Rev.* 71:1047–1080.

Patlak, J. B., and M. Ortiz. 1985. Slow currents through single sodium channels of the adult rat heart. *J. Gen. Physiol.* 86:89–104.

Patlak, J. B., and M. Ortiz. 1986. Two modes of gating late Na^+ channel currents in frog sartorius muscle. *J. Gen. Physiol.* 86:305–326.

Patlak, J. B., and M. Ortiz. 1989. Kinetic diversity of Na^+ channel bursts in frog skeletal muscle. *J. Gen. Physiol.* 94:279–301.

Patlak, J. B., M. Ortiz, and R. Horn. 1986. Open time heterogeneity during bursting of sodium channels in frog skeletal muscle. *Biophys. J.* 49: 773–777.

Pietrobon, D., and P. Hess. 1990. Novel mechanism of voltage-dependent gating in L-type calcium channels. *Nature.* 346:651–655.

Saint, D. A., Y. K. Ju, and P. W. Gage. 1992. A persistent sodium current in rat ventricular myocytes. *J. Physiol. (Lond.).* 453:219–231.

Sokabe, M., F. Sachs, and Z. Jing. 1991. Quantitative video microscopy of patch clamped membranes. Stress, strain, capacitance, and stretch channel activation. *Biophys. J.* 59:722–728.

Sorbera, L. A., and M. Morad. 1991. Modulation of cardiac sodium channels by cAMP receptors on the myocyte surface. *Science.* 253:1286–1289.

Stühmer, W., and W. Almers. 1982. Photobleaching through glass micropipettes: sodium channels without lateral mobility in the sarcolemma of frog muscle. *Proc. Natl. Acad. Sci. USA.* 79:946–950.

Sunami, A., Z. Fan, F. Nakamura, M. Naka, T. Tanaka, T. Sawanobori, and M. Hiraoka. 1991. The catalytic subunit of cyclic AMP-dependent protein kinase directly inhibits sodium channel activities in guinea-pig ventricular myocytes. *Pflügers Arch.* 419:415–417.

Wellis, D., L. J. DeFelice, and M. Mazzanti. 1990. Outward Na current in beating heart cells. *Biophys. J.* 57:41–48.

West, J. W., R. Numann, B. J. Murphy, T. Scheuer, and W. A. Catterall. 1991. A phosphorylation site in the Na^+ channel required for modulation by protein kinase C. *Science.* 254:866–868.

Yue D. T., J. H. Lawrence, and E. Marban. 1989. Two molecular transitions influence cardiac sodium channel gating. *Science.* 244:349–352.